

## **General Disclaimer**

### **One or more of the Following Statements may affect this Document**

- This document has been reproduced from the best copy furnished by the organizational source. It is being released in the interest of making available as much information as possible.
- This document may contain data, which exceeds the sheet parameters. It was furnished in this condition by the organizational source and is the best copy available.
- This document may contain tone-on-tone or color graphs, charts and/or pictures, which have been reproduced in black and white.
- This document is paginated as submitted by the original source.
- Portions of this document are not fully legible due to the historical nature of some of the material. However, it is the best reproduction available from the original submission.



LOW FREQUENCY THERMOMECHANICAL SPECTROMETRY OF  
POLYMERIC MATERIALS: TACTIC POLYMETHYLMETHACRYLATES

S. J. Stadnicki and J. K. Gillham  
Department of Chemical Engineering

and

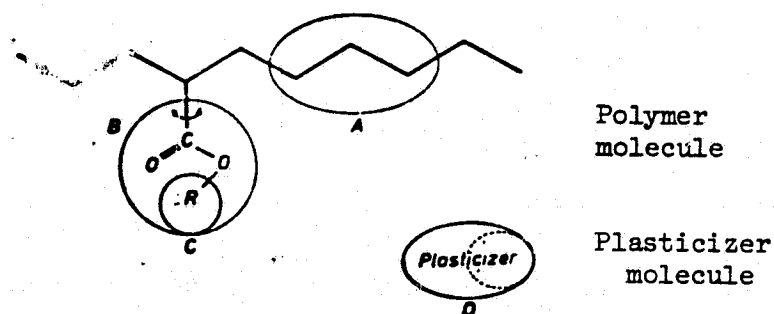
Y. Hazony  
Department of Civil Engineering  
Princeton University  
Princeton, New Jersey 08540

SYNOPSIS

A computerized and automated torsional pendulum has been used to characterize amorphous polymethylmethacrylates at about 1 Hz in the temperature sequence  $473 \rightarrow 93 \rightarrow 473^\circ\text{K}$ . The effects of thermal pre-history, temperature cycling, water content and tacticity are demonstrated. In particular, a comparison of the out-of-phase shear modulus ( $G''$ ) versus temperature for "syndiotactic", "atactic" and "isotactic" polymer specimens shows that the intensity of the glassy-state  $\beta$  loss peak decreases with increasing isotactic content while the temperature of its location remains the same. Extrapolation suggests that completely isotactic polymer would not display a  $\beta$  loss peak. The shape and location of the  $G''$  data at low temperatures indicate that the basic mechanism of the  $\beta$  process is the same for the three polymer samples and supports the validity of the extrapolation. The effect of tacticity is reflected also in the glass transition region; the isotactic sample has its  $T_g$  about  $65^\circ\text{C}$  lower with greater intensity than the syndiotactic polymer.

## INTRODUCTION

Solid state transitions in polymeric materials have been associated with the onset of sub-molecular motions of the polymer chains. Although these have been considered to be intramolecular in general, the local environment of the polymer molecule can exert a strong influence through, for example, the effects of crystallinity, polarity and diluents (1). The manner of specimen preparation and previous history can also affect transitions. The transitions can be considered to arise when sufficient free volume is available to permit the occurrence of these side chain and backbone reorientations (2). The glass transition is the principal transition of amorphous polymeric materials and is associated with the onset of long range segmental motion of the polymer backbone. The various types of shorter range motion occurring below the glass transition have been catalogued (3) and are represented below:



Type A. Localized motion within the polymer backbone.

Type B. Oscillation of the side group about the bond linking it to the main chain.

Type C. Internal motion within the side group with no obstruction from the main chain.

Type D. Motion of small plasticizer molecules embedded in the glassy matrix.

Chain-end motion, especially in low molecular weight polymers, may also give rise to secondary transitions.

Polymethylmethacrylate (PMMA) provides an example of the variety of molecular motions which occur in amorphous polymeric materials. Dynamic mechanical studies have shown that PMMA exhibits four solid state transitions which have been attributed (in order of increasing temperature) to the following: methyl ester motion,  $\alpha$ -methyl motion, side chain rearrangement coupled perhaps with localized backbone motion, and long range backbone motion of the main polymer chain (1,4,5). A transition ( $T_{ll} > T_g$ ) separates the "fixed fluid" state from a "true liquid" state above the glass transition (6,7,8). As a general rule, the temperature for the onset of motion increases with increasing size of the moving entity. In addition to dynamic mechanical studies, research in this area has included wide-line nuclear magnetic resonance (NMR) and dielectric structure-property correlations on homopolymers and copolymers. Although a majority of the work on the relaxation behavior of PMMA has utilized samples which are either atactic or uncharacterized with respect to microtacticity content, the literature reports unusual differences between isotactic and syndiotactic forms which have not been unambiguously explained. These include the effect of tacticity on the glass transition, the formation of a stereocomplex upon mixing syndiotactic and

isotactic methylmethacrylate polymers (9,10) and the stereospecific matrix ("replica", "template") polymerization of syndiotactic PMMA in the presence of isotactic PMMA (11,12).

In this communication three characterized samples of amorphous polymethylmethacrylates with varying tacticity were examined by torsional braid analysis [TBA (13)] at about 1 Hz in the temperature range 473° to 93°K, using an automated and computerized instrument (13-17). The development of the methodology of the hierarchical computer network used for data acquisition and reduction has been described (16). Procedures used in the reduction of experimental data are summarized in the Appendix. The present paper reports effects of modes of data presentation, prehistory, temperature cycling, moisture level, and tacticity. The effect of molecular weight in the temperature region,  $T > T_g$  is also discussed.

## EXPERIMENTAL

### Materials

Three characterized "syndiotactic", "atactic", and "isotactic" samples of polymethylmethacrylate were examined using an automated TBA instrument. Manually reduced TBA data for the same polymers, together with documentation of their syntheses, average molecular weights ( $\bar{M}_w$  and  $\bar{M}_n$ ) and tactic contents (syndio-, hetero-, and iso-) have been reported (18). Characteristics of the stereoregular polymethylmethacrylates are summarized in Table I which includes assignments for the  $T_g$  and  $T_\beta$  transitions made on the basis of the present data. Although the overall tactic content of each of the samples is known, the extent of the "blocky" character is not.

### Procedure

Polymer-braid composite specimens were prepared by impregnating multifilamented glass braids (length, 8 inches) in 10 percent solutions of the polymers (g. polymer/100 ml. solvent) in tetrahydrofuran (THF, b.p. 66°C). Solvent was removed by heating the composite specimens to 473°K at the rate of 2°K/minute in flowing dry nitrogen gas (obtained from a sealed Dewar of liquid nitrogen). The thermomechanical spectra were then obtained in a nitrogen atmosphere while cooling the solvent-free composite specimens to 93°K and then heating to 473°K at a rate of 2°K/minute. Data are presented for the cooling mode unless otherwise noted. Numerical values which are proportional to the in-phase and out-of-phase shear moduli were determined for the composite specimens. Interpretation of the thermomechanical spectra in terms of the behavior of the polymeric material is based on the substrate being inert. Thermogravimetric analysis (TGA) indicated that the polymers were stable below 200°C in the time scale of the experiments (18).

Attempts to crystallize these samples of PMMA by annealing below the reported melting temperatures [ $T_m$  (isotactic) = 160°C (19),  $T_m$  (syndiotactic) > 200°C (19)] were unsuccessful (18). That isotactic and syndiotactic polymers do not crystallize with ease has been reported (20).

### Modes of Data Presentation

The spectra for the syndiotactic, atactic, and isotactic polymethylmethacrylate specimens<sup>recorded</sup> on cooling, are presented in Figures 1, 2 and 3, respectively, in terms of the temperature dependence of the relative rigidity,  $1/P^2$ , [which is a good approximation (16) for the relative

elastic shear modulus,  $G'$ ] and logarithmic decrement,  $\Delta$ .  $P$  is the period of the damped oscillations in seconds;  $\Delta \equiv \log_e A_i/A_{i+1}$ , where  $A_i$  is the maximum angular displacement of the  $i^{\text{th}}$  oscillation. This is a conventional mode for presentation of torsional pendulum data. Figures 4-6 illustrate the same data in terms of  $K''G''$  and  $K'dG'/dT$  versus temperature,  $^{\circ}\text{K}$ , for both cooling and heating. In this report  $K'G'$  is defined as  $(\alpha^2 + \omega^2)$  and  $K''G''$  as  $2\alpha\omega$ , where  $\alpha$  is the damping coefficient and  $\omega$  is the frequency of oscillations in radians per second (which is equal to  $2\pi/P$ ).  $K''$  and  $K'$  are constants which depend on the geometry of the pendulum and are omitted in further discussion. Plots of  $G''$  and  $dG'/dT$  versus  $T$  have been displaced vertically by arbitrary amounts for purposes of presentation. This second mode of data presentation is seen to be internally consistent for the assignment of transition temperatures for PMMA in contrast to the mode of data presentation in Figures 1, 2 and 3. A summary of the transition temperatures for the three PMMA samples as determined from the maxima of the various modes of data exposition is provided in Table II. The assignment of transition temperatures appears to conform to the following trend for both  $T_g$  and  $T_\beta$ :

$$T(\tan\delta) = T(\Delta) \geq T(\alpha) \geq T(G'') = T(dG'/dT).$$

Use of  $G''$  rather than other loss parameters appears to be particularly effective for investigating glassy-state transitions by reducing the response of the  $T_g$  relaxation. The  $G''$  mode would also appear to be the logical function to use in comparing dynamic mechanical and dielectric loss ( $\epsilon''$ ) data. Another advantage in its use appears to lie in the flat baseline

of  $G''$  versus temperature curves which could provide opportunities for comparing peak shapes and for resolving peaks quantitatively.

## RESULTS

### Effect of Tacticity on Transitions

The general characteristics of the TBA spectra (Figures 1-6) compare well with published work (21), in exhibiting two distinct loss peaks above  $93^\circ\text{K}$ . The glass transition temperatures (as determined from  $G''$  and  $dG'/dT$  data) are assigned using the sharp loss peaks at  $399^\circ\text{K}$  (0.68 Hz),  $384^\circ\text{K}$  (0.67 Hz), and  $334^\circ\text{K}$  (0.81 Hz) in syndiotactic, atactic, and isotactic PMMA, respectively. Each loss peak is accompanied by a large rise in rigidity with decreasing temperature. The glassy-state loss peaks ( $\beta$ -peaks) in syndiotactic and atactic PMMA are broad and centered at  $292^\circ\text{K}$  (1.25 Hz) and  $297^\circ\text{K}$  (1.24 Hz), respectively. The  $\beta$  relaxation in isotactic PMMA is ill-defined and appears as a shoulder at around  $280^\circ\text{K}$  (1.4 Hz). Below  $T_g$  the shape of the loss spectrum for all three polymers is the same. The  $\beta$ -peak for each of these polymers is accompanied by a small but distinct rise in the rigidity with decreasing temperature. This rise is less pronounced for the isotactic than for the atactic and syndiotactic polymers. The absolute value of the relative rigidity at low temperatures ( $\sim 93^\circ\text{K}$ ) is about the same for the three specimens; this indicates the presence of an approximately equal amount of polymer in each composite specimen. Absence of crystallinity (as noted above) is indicated by the high degree of reversibility of data with temperature cycling for  $T > T_g$  (Figures 4-6). Thermohysteresis effects (irreversibilities) arise in

(semi-) crystalline polymers due to temperature differences between crystallizing and melting.

The similarity of the thermomechanical spectra of atactic and syndiotactic PMMA for the glassy state was not unexpected due to the small differences in microtacticity (51% versus 70% syndiotacticity). Above  $T_g$  the loss and rigidity curves for the isotactic polymer are nearly flat whereas the loss curves rise and the rigidity curves drop at about 160°C for the syndiotactic and atactic polymers. Differences above  $T_g$  for the polymers are attributed to the effect of molecular weight on the flow transition,  $T_{ll}$ .

#### Effect of Prehistory

A problem of concern is the determination of suitable conditioning parameters for the preparation of specimens. To obtain the relaxation spectrum of a polymer *per se*, it is necessary to prepare the specimen in a manner which removes all occluded volatiles (e.g., solvent and absorbed moisture) without causing degradation. Thermogravimetric analysis (TGA), often used to complement thermomechanical spectrometry, is employed to determine temperature regions in which weight loss occurs. A more informative approach determines the volatile components formed on heating by employing, for example, a pyrolyzer in series with a gas chromatograph (22) and an infrared spectrophotometer (23).

Thermogravimetric analysis of the isotactic sample showed a 1-2% weight loss in heating to 473°K after predrying to 423°K. Molecular weight chromatographic analysis (22) of the volatile products of heating in the 423° to 473°K range indicated one major volatile component having a molecular

weight of about 93. Monomer was not detected until above 523°K. A check of the synthesis procedure (18) indicated that one of the solvents used for purification was probably the volatile component in question.

The thermomechanical spectra (logarithmic decrement versus temperature) of a single specimen of the syndiotactic PMMA after preheating first to 423°K and then to 473°K, respectively, at the rate of 2°K/minute are shown in Figure 7. The glass transition temperature of the specimen<sup>which was</sup> dried more thoroughly is some 11 degrees higher. The secondary transition (298°K) does not appear to have been affected, but the observed differences in the loss levels at temperatures between  $T_{\beta}$  and  $T_g$  and also at  $\sim 100^{\circ}\text{K}$  are attributed to the presence of the small amount of diluent.

#### Effect of Thermal Cycling

The thermomechanical spectra for the syndiotactic PMMA, preheated to 473°K, are displayed in Figure 8 for cooling to 93°K and subsequent heating to 473°K at 2°K/minute. The thermo-hysteresis in the  $G''$  loss data at low temperatures may be due either to inaccurate temperature assignment (thermal lag between the thermocouples and specimen) or to microcracking of the composite specimen. A portion of the elastic shear modulus curve,  $G'$ , (shown in Figure 8) is displayed on an expanded linear scale in Figure 9. [An inadvertent experimental gap exists in the data above 330°K.] The irreversibility in the rigidity, upon first cooling to 93°K and then heating, is attributed to microcracking of the composite specimen. The mechanism leading to these cracks may involve thermal stresses which arise from the different coefficients of contraction of the two phases of the specimen. Polymers with bulky side

groups are observed to be susceptible to cracking (18) probably because of the weaker cohesive forces between chains, per unit cross-sectional area, than for more compact molecules (24, 25). The fracture mechanism may also involve penetration of trace amounts of water into small pores and its subsequent expansion upon freezing. The moisture content of the "dry" nitrogen atmosphere was measured to be about 5 parts per million (ppm) which corresponds to a frost point of about 207°K. In a similar manner, occluded diluent could form voids upon freezing which could be sites for initiation of cracks. Alternatively, cracks may originate from the stress applied to initiate pendulum oscillations, particularly at low temperatures where side group motions are frozen out. In any case, the loss level would be expected to be higher after a crack, reflecting an increase in the ability of the composite specimen to dissipate energy on deformation. In a like manner, the elastic modulus curve would be expected to be at a lower level on heating after cracking, indicating a less rigid structure. Indeed, this is observed.

#### Effect of H<sub>2</sub>O

Specimens of atactic PMMA were prepared from 10% solutions of the polymer in THF, heated to 473°K at 2°K/minute and cooled to room temperature in a flowing dry nitrogen atmosphere. The specimens were then conditioned overnight at room temperature in a flowing nitrogen atmosphere containing known amounts of water. A hygrometer (Panametrics Model 2000 with a calibrated P2 gas probe) capable of measuring to less than 1 ppm, was used to monitor the water content continuously at the exit port of the TBA apparatus. The hygrometer utilizes a humidity sensor which is essentially an aluminum oxide capacitor, the impedance of which varies directly with

the water vapor pressure.

The effect of six different levels of humidity on the thermomechanical spectra of atactic PMMA was examined. The water contents of these experiments were in parts per million: 10, 300, 1000, 2500, 5000, and 10,000. The last figure corresponds to a relative humidity level of 100% at a temperature of about 7°C. After conditioning in the controlled atmospheres the specimens were taken through the temperature cycle 293 → 473 → 93 → 473°K at 2°K/minute. The "humid" conditioning atmosphere was changed to a flowing dry atmosphere, containing less than 5 ppm H<sub>2</sub>O, at 303°K during the cooling mode. The presence of water vapor showed no effect on T<sub>g</sub>, but a small "γ-peak" centered around 170°K was detectible for conditioning levels of ≥ 300 ppm. This is illustrated in Figure 10 which shows the thermomechanical loss spectra for three atactic PMMA specimens conditioned at 300, 2500, and 10,000 ppm of water vapor. Data shown is for 473 → 93°K. The reversibility of the data through this "water transition" is illustrated in Figure 11 for the atactic specimen conditioned at 10,000 ppm. A γ-peak in atactic PMMA at about -100°C (1 Hz) due to absorbed moisture has been reported (21).

### DISCUSSION

The discussion is divided into three sections which correspond to three regions of thermomechanical behavior: , T<sub>g</sub>, T > T<sub>g</sub>, and T<sub>β</sub>.

#### T<sub>g</sub>

The glass transition temperature, T<sub>g</sub>, represents the onset of main-chain segmental motion and is revealed mechanically by maxima in the loss

( $G''$ ) and in the derivative of the rigidity ( $dG'/dT$ ) curves. Many factors influence the temperature location of  $T_g$ , but among the most basic is molecular flexibility (ease of conformational change) which is affected by the type of substituent. However, much of the knowledge concerning  $T_g$  is empirical and it is difficult to separate intermolecular from intramolecular contributions.

From the present data the glass transition temperature of the isotactic PMMA is observed to be  $65^\circ\text{C}$  lower and the magnitude of the loss peak considerably greater than that of the syndiotactic form (Figure 12).

$T_g$  of the atactic sample is between those of the isotactic and syndiotactic samples both in temperature and magnitude. The

molecular weight of the isotactic sample is about 30 times that of both the syndiotactic and atactic forms which, if at all, should have the effect of raising the glass transition temperature.

Early attempts to explain the large difference in the glass transition temperatures between isotactic and syndiotactic forms invoked intramolecular chain stiffness as the controlling factor (21). That the syndiotactic chain is somewhat stiffer and thus gives rise to the higher  $T_g$  is supported by theoretical studies of molecular models, and by dilute solution properties measured by dielectric and high resolution NMR techniques (26, 27, 28). It should be noted that arguments based on solution properties utilize only intramolecular factors. Attempts to apply these conclusions to the solid state should be exercised with caution. In fact, measurements of  $\theta$ -dimensions and small angle X-ray scattering data are reported to show that the flexibility difference between the tactic configurations is so small that it cannot be the main reason for the large difference in the values of the glass transitions (18, 29).

This sets the stage for proposing an intermolecular argument. Geometrical intermolecular interlocking of the side chains has been proposed as a mechanism whereby the glass transition can be increased (30, 31). This was held responsible for the higher glass transition of the syndiotactic polymer (18). The chain entanglement concept differs in involving

a long range chain-looping effect. On the other hand, it was suggested that the side chain configuration of the isotactic PMMA does not permit such interlocking sites. Intermolecular dipole-dipole associations between the highly polar side chains in PMMA may magnify geometrical effects.

A further point to be considered is that the density of the isotactic form is greater than that of the syndiotactic form in the amorphous state at room temperature (18). Packing is therefore more efficient in the isotactic form. This does not necessarily mean that the glass transition temperature of the isotactic form should be greater than the syndiotactic, as could be inferred from free volume arguments. The shape as well as the fraction of free volume is important. Molecules may pack efficiently for geometrical reasons with minimal interunit binding forces (18). The lower density of the syndiotactic form at room temperature presumably stems from its greater softening in the  $\beta$ -transition region as is reflected in the rigidity curve in Figure 13. This in turn is a consequence of the greater activity of the ester linkages in the syndiotactic material prior to the glass transition as is reflected in the loss curves in Figure 12.

$T > T_g$

The  $T_{\ell\ell}$  ( $> T_g$ ) transition (6,7,8) separates two regions of flow designed "fixed fluid" ( $T_g < T < T_{\ell\ell}$ ) and "true liquid" ( $T > T_{\ell\ell}$ ) on the

basis of rheological behavior. It is a function of molecular weight. From the present data, the syndiotactic and atactic samples appear to be low enough in molecular weight to give indications of  $T_{\ell\ell}$  transitions (at temperatures in excess of  $200^{\circ}\text{C}$ ). This is seen both in an increase in the loss curves (e.g., Figure 12) and in a corresponding decrease in the rigidity curves (e.g., Figure 13) about  $160^{\circ}\text{C}$ .

The high molecular weight isotactic sample shows no indication of a  $T_{\ell\ell}$  transition below  $200^{\circ}\text{C}$ ; the rigidity above the glass transition temperature is relatively flat and higher in magnitude than for the syndiotactic form. This is indicative of an extensive rubbery plateau region with little or no rubbery flow to at least  $200^{\circ}\text{C}$ . The response of an isotactic sample (95% isotactic,  $\bar{M}_V = 6 \times 10^5$ ) between  $T_g$  and  $160^{\circ}\text{C}$  for small strains was found to be completely elastic (32) (creep and creep recovery experiments at  $159^{\circ}\text{C}$  were identical and no permanent flow was observed). Presumably the  $T_{\ell\ell}$  transition for this molecular weight was above  $160^{\circ}\text{C}$ .

### $T_{\beta}$

Polymeric materials exhibit secondary relaxations below the glass transition which have been correlated with the motion of very short main chain segments or side groups. The temperature locations of these loss peaks are for the most part determined by intramolecular potential energy barriers (3). The existence and location of secondary transitions are of theoretical and practical importance since for many polymers these relaxations have been associated with important changes in macroscopic properties (33-35). For example, a glassy-state transition at low temperatures appears to be

necessary for good impact strength of glassy polymeric materials at room temperature. However, it is not a sufficient condition (33).

The most prominent glassy-state transition in PMMA is the  $\beta$ -transition. Other secondary transitions (attributed to  $\alpha$ -methyl and ester methyl motions) have been observed by other workers to occur at temperatures below the <sup>presently-used</sup> operating range of the TBA apparatus (at about 1 Hz). The  $\beta$ -transition in PMMA has been attributed to the onset of side chain motion on the basis of comparative studies using wide line NMR, dielectric, and mechanical measurements (21, 36, 37). However, the detailed mechanism of the molecular relaxation is not understood and, in particular, it is not clear to what extent localized motions of the main chain are involved. The  $T_{\beta}/T_g$  ( $^{\circ}\text{K}/^{\circ}\text{K}$ ) ratio has been suggested to reflect the extent of coupling that exists between the two transitions (35): for many amorphous polymers the empirical ratio determined mechanically is about 0.75 at about 1 Hz. The values for the syndiotactic and isotactic polymethylmethacrylates of the present work are 0.74 and  $> 0.84$ , respectively. High coupling in the isotactic polymer is also revealed by the increase in intensity of the  $T_g$  loss peak parallelling the decrease in intensity of the  $\beta$ -peak with increasing isotacticity.

The present results (Figures 12 and 13) show that the  $\beta$ -transition in syndiotactic PMMA is highly pronounced whereas it is almost absent in the isotactic material. The atactic material has intermediate properties. Similar shapes for the three loss curves at low temperatures are noted. The rigidity spectra show minor softening of the isotactic specimen in the temperature region of the  $\beta$ -transition. This is consistent with the density of isotactic samples being greater than the syndiotactic form at room temperature, in spite of the isotactic polymer being closer to its glass transition.

The higher molecular weight of the isotactic sample should not significantly affect the temperature and intensity of the  $\beta$ -transition.

The  $\beta$ -transition is almost absent in the 91% isotactic specimen and it is suggested that there will be no  $\beta$ -transition for a 100% isotactic polymer. The shape and location of the thermomechanical loss spectra at low temperatures for the isotactic and syndiotactic forms are similar; this indicates a similar molecular mechanism and supports the projection. Heterotactic impurities are assumed to be responsible for the weak  $\beta$ -transition in the 91% isotactic PMMA in which the isotactic side groups are immobilized.

Quantitative analysis of the shape and areas of the loss ( $G''$ ) peaks in the temperature region of the  $\beta$ -transition for the present PMMA samples has shown that only the heterotactic and syndiotactic components contribute to the

$\beta$ -transition (38). The numerical values are consistent with the quantitative characterization of each sample by NMR (Table I).<sup>^</sup> It follows that the  $\beta$ -process is essentially intramolecular in character for polymethylmethacrylate. Although

<sup>^</sup> intermolecular steric hindrance decreases the intensity of secondary loss maxima in polymers sometimes without change of temperature (39), the above results indicate that this is not the important factor in the  $\beta$ -mechanism of isotactic PMMA, but it would account for its higher density at room temperature.

The absence of a  $\beta$ -peak is noted for polyisobutylene,  $[\text{CH}_2\text{C}(\text{CH}_3)_2]$ , which also has an anomalously low glass transition temperature (31). The latter has been attributed to a lack of spacial sites for geometrical intermolecular interlocking along the molecules (30) and this reason may be a factor contributing to the low  $T_g$  of isotactic polymethylmethacrylate (18). However, amorphous isotactic polystyrene, which does not show a  $\beta$ -peak, has a glass transition comparable to that of atactic polystyrene (40, 41). Thus, the absence of a  $\beta$ -transition does not necessarily affect the mechanism of the glass transition.

in solution, albeit probably over short distances (46). Conformational analyses and infrared measurements have determined that the molecular structure is the 5/1 helix in crystalline isotactic PMMA (47). Conformational analysis has also shown that for the 5/1 and 5/2 crystalline forms of isotactic PMMA, the energy barrier for rotation of the side group is so high as to prohibit rotation (44, 47). Moreover isotactic PMMA in solution may exist either as the 5/1 or 5/2 helix (46,49). This implies that isotactic PMMA can assume a local helical conformation even in the amorphous glassy state (42).

The same conclusion has been surmized from the observation that the polymer could crystallize to a 5/2 helix with little or no change in density (43). It appears that the tactic spatial arrangement of side groups in the helical conformation of isotactic PMMA could account for some of the unusual properties of this polymer:

- (1) The absence of side chain motion for a 100% isotactic sample (due to immobilized ester groups in the helical conformation).
- (2) The stereospecific "replica" polymerization mechanism.
- (3) The stereocomplex formation with syndiotactic PMMA in solution.
- (4) The higher degradation temperature of the isotactic as compared with syndiotactic and atactic PMMA (18).

PREVIOUS PAGE BEING NOT FILMED

## APPENDIX

The data in these experiments were acquired and processed using a hierarchical computer system. Independent analog devices were used to control the sequencing and temperature programming of the experiments. An IBM System/7 computer was used for on-line acquisition, preprocessing, and transmission of the data to disc storage on an IBM 370/158 computer). At the end of an experiment the data were transferred to IBM 360/91 batch computer for final processing.

### PREPROCESSING

Preprocessing is used to standardize and reduce the volume of data being sent to the batch computer for final analysis. In this step, a set number of data points are acquired at a calculated scan rate. The scan rate is automatically determined from the <sup>estimated</sup> period of oscillation of the torsional pendulum to ensure that at least two complete cycles will be acquired for final data processing. At the time of these experiments the data preprocessing step had not been optimized. For convenience 640 data points (2 buffers) were acquired at a typical scan rate of 100 points/sec. Indications are that many less points are actually needed.

In addition to the above, boundary conditions were imposed to force the preprocessed data to begin on the first positive peak below a set voltage level (2 volts). Local maxima due to noise were checked for by using a digital filtering technique. This technique tested the next 10 points following a suspected maximum for absolute value and slope change.

### PROCESSING

The basic equation of motion for a simple torsional pendulum is,

$$I \frac{d^2\theta}{dt^2} + \eta_{dym} \frac{d\theta}{dt} + G_{dym} \theta = 0 \quad (1)$$

where  $\theta$  is the angle of displacement from the neutral position (or the amplitude of the electrical analog),  $I$  is an inertial constant,  $\eta_{dym}$  is the dynamic viscoicity, and  $G_{dym}$  is the dynamic modulus.

The solution to Eq.(1) has the form of an exponentially damped cosine function

$$\theta = \theta_0 e^{-\alpha t} \cos(\omega t + \phi) \quad (2)$$

with

$$\alpha = \eta_{dym}/2I$$

and

$$\omega = [(G_{dym}/I) - (\eta_{dym}/2I)^2]^{1/2}$$

where  $\alpha$  is the damping coefficient and  $\omega$  is the frequency in radians per second. A phase angle term,  $\phi$ , has been introduced because of the timing of the initiation of data acquisition.

A torsional braid specimen has a tendency to change its rotational orientation through the course of an experiment due to stresses caused by volume expansion and contraction. This in turn causes an approximately linear drift in the baseline of the damped sinusoid. This is represented by:

$$\theta = \theta_0 e^{-\alpha t} \cos(\omega t + \phi) + \beta t + C \quad (3)$$

where  $\beta$  is the slope of the drift and  $C$  is the offset.

The differential equation corresponding to Eq.(3) is the one used in the final processing of the digitized data; i.e.,

$$\frac{d^2\theta}{dt^2} + 2\alpha \frac{d\theta}{dt} + (\alpha^2 + \omega^2) \theta - C(\alpha^2 + \omega^2) - 2\alpha\beta - \beta(\alpha^2 + \omega^2)t = 0 \quad (4)$$

which may be simplified to

$$D = \frac{d^2\theta}{dt^2} + A_1 \frac{d\theta}{dt} + A_2 \theta + A_3 t + A_4 = 0 \quad (5)$$

where  $A_i$  ( $i = 1, 2, 3$  &  $4$ ) are the parameters fitted by a linear least mean squares analysis, and

$$\alpha = A_1/2$$

$$\omega = [A_2 - (A_1/2)^2]^{1/2}$$

(The significance of D will be discussed below.) The derivative values of  $\theta$  at any point n are calculated numerically from an extension of Newton's Forward Formula, which utilizes 5 consecutive points to obtain the first and second derivatives.

$$\frac{d\theta}{dt}_n = (-\theta_{n+2} + 8\theta_{n+1} - 8\theta_{n-1} + \theta_{n-2})/12h \quad (6)$$

$$\frac{d^2\theta}{dt^2}_n = (-\theta_{n+2} + 16\theta_{n+1} - 30\theta_n + 16\theta_{n-1} - \theta_{n-2})/12h^2 \quad (7)$$

where h is the step size.

The linear least mean squares fitting of N experimental data to the differential form of the equation of motion involves minimization of the summation,

$$S = \sum_{n=3}^{N-2} v_n^2 = \sum_{n=3}^{N-2} (f_n - D_n)^2 \quad (8)$$

where  $v_n^2$  are the squares of the approximation errors and  $f_n$  is derived from the experimental data,

$$f_n = \frac{d^2\theta_n}{dt_n^2} + A_1 \frac{d\theta_n}{dt_n} + A_2\theta_n + A_3t_n + A_4 \quad (9)$$

The respective derivatives are defined by Eqns. 6 and 7.  $t_n$  is  $n$  divided by the scan rate.  $D_n$  is identically zero by definition (Eqn.5). The limits of the summation ( $n=3$  to  $N-2$ ) have been dictated by the method for obtaining the derivatives. From the requirement that  $S$  is minimized, it follows that,

$$\frac{\partial S}{\partial A_i} = 2 \sum_n v_n \frac{\partial v_n}{\partial A_i} = 0 \quad (i=1 \text{ to } 4) \quad (10)$$

This results in four simultaneous linear equations which may be presented in matrix notation:

$$\begin{bmatrix} \sum_n \dot{\theta}_n^2 & \sum_n \dot{\theta}_n \theta_n & \sum_n \dot{\theta}_n & \sum_n \dot{\theta}_n t_n \\ \sum_n \dot{\theta}_n \theta_n & \sum_n \theta_n^2 & \sum_n \theta_n & \sum_n \theta_n t_n \\ \sum_n \dot{\theta}_n & \sum_n \theta_n & \sum_n 1 & \sum_n t_n \\ \sum_n \dot{\theta}_n t_n & \sum_n \theta_n t_n & \sum_n t_n & \sum_n t_n^2 \end{bmatrix} \begin{bmatrix} A_1 \\ A_2 \\ A_3 \\ A_4 \end{bmatrix} = \begin{bmatrix} - \sum_n \ddot{\theta}_n \dot{\theta}_n \\ - \sum_n \ddot{\theta}_n \theta_n \\ - \sum_n \ddot{\theta}_n \\ - \sum_n \ddot{\theta}_n t_n \end{bmatrix}$$

The above expression is solved by a matrix inversion procedure to determine the values of the coefficients  $A_i$ .  $A_1$  and  $A_2$  contain the damping and frequency parameters (see above).

The data processing was further refined by limiting the analysis to an integral number of cycles. Effectively this is a digital filtering technique which was empirically found to improve the signal-to-noise level. Frequency, damping, and the number of points comprising the maximum number of integral cycles are determined by an iterative process which typically converges after 3 sequences. Computer simulations have demonstrated that this operation is theoretically unnecessary for noise-free data.

ACKNOWLEDGMENT

This work was supported by the National Aeronautics and Space Administration (Grant NGR 31-001-221) and the Chemistry Branch of the Office of Naval Research. Appreciation is expressed also to Dr. E. Gipstein, International Business Machines Corporation, San Jose, California, for providing the characterized polymers.

1. J. A. Sauer, *J. Polym. Sci.*, 32C, 69 (1971).
2. M. C. Shen and A. Eisenberg, *Rubber Chem. Technology*, 43, 95 (1970).
3. J. Heijboer, *Secondary Mechanical Transitions and Chemical Structure of Amorphous Polymers*, Centraal Laboratorium TNO, Delft, The Netherlands, 1973.
4. I. M. Ward, *Mechanical Properties of Solid Polymers*, Chapter 8, Wiley-Interscience, London, 1971.
5. S. G. Turley and H. Keskkula, *J. Polym. Sci.*, Part C, 14, 69 (1966).
6. S. J. Stadnicki, J. K. Gillham and R. F. Boyer, *J. Appl. Polym. Sci.*, in press.
7. C. A. Glandt, H. K. Toh, J. K. Gillham and R. F. Boyer, *J. Appl. Polym. Sci.*, in press.
8. J. K. Gillham, J. A. Benci and R. F. Boyer, *J. Appl. Polym. Sci.*, in press.
9. A. M. Liquori, G. Anzuino, V. M. Coiro, M. D'Alagni, P. DeSantis and M. Savino, *Nature*, 206, 358 (1965).
10. J. Špěváček and B. Schneider, *Makromol. Chem.*, 175, 2939 (1974).
11. T. Miyamoto and H. Inayaki, *Polymer J.*, 1(1), 46 (1970).
12. R. Buter, Y. Y. Tan and G. Challa, *J. Polym. Sci.-Chem.*, 11, 989 (1973).
13. J. K. Gillham, *A.I.Ch.E. Journal*, 20(6), 1066 (1974).
14. C. L. M. Bell, J. K. Gillham and J. A. Benci, *Society of Plastics Engineers, Technical Papers*, 20, 598 (1974).
15. Y. Hazony, S. J. Stadnicki and J. K. Gillham, *American Chemical Society, Polymer Preprints*, 15(1), 549 (1974).
16. S. J. Stadnicki, J. K. Gillham and Y. Hazony, *American Chemical Society, Polymer Preprints*, 15(1), 556 (1974).
17. J. K. Gillham, S. J. Stadnicki and Y. Hazony, *American Chemical Society, Polymer Preprints*, 15(1), 562 (1974).
18. E. Kiran, J. K. Gillham and E. Gipstein, *J. Macromolecular Science-Physics*, B9(2), 341 (1974).
19. T. G. Fox, B. S. Garrett, W. E. Goode, S. Gratch, J. F. Kincaid, A. Spell and J. D. Stroupe, *J. Am. Chem. Soc.*, 80, 1768 (1958).
20. W. E. Goode, F. H. Owens, R. P. Fellmann, W. H. Snyder and J. E. Moore, *J. Polym. Sci.*, 46, 317 (1960).
21. N. G. McCrum, B. E. Read and G. Williams, *Anelastic and Dielectric Effects in Polymeric Solids*, John Wiley & Sons, New York, 1967, Chapter 8.

22. E. Kiran and J. K. Gillham, *J. Macromol. Sci.-Chem.*, A8(1), 211 (1974).
23. H. H. Kuo, H. Pfeffer and J. K. Gillham, *American Chemical Society, Organic Coatings and Plastics Chemistry Division*, 35(1), 434 (1975).
24. P. I. Vincent, *Nature*, 233(40), 104 (1971).
25. P. I. Vincent, *Polymer*, 13, 588 (1972).
26. H. A. Pohl, R. Bacskai and W. P. Purcell, *J. Phys. Chem.*, 64, 1701 (1960).
27. S. Brownstein and D. M. Wiles, *Can. J. Chem.*, 44, 153 (1966).
28. F. P. Grigoreva and Y. Y. Gotlib, *Polym. Sci. USSR*, 10, 356 (1968).
29. R. G. Kriste, *Makromol. Chem.*, 101, 91 (1967).
30. J. R. Martin and J. K. Gillham, *J. Appl. Poly. Sci.*, 16, 2091 (1972).
31. A. Hiltner, E. Baer, J. R. Martin and J. K. Gillham, *J. Macromolecular Science-Physics*, B9(2), 255 (1974).
32. D. J. Plazek and N. Raghupathi, *American Chemical Society, Polymer Preprints*, 15, (1), 53 (1974).
33. R. F. Boyer, *Polym. Engineering Sci.*, 8, 161 (1968).
34. J. Heijboer, *J. Polym. Sci.*, C7, 3755 (1968).
35. R. F. Boyer, *Multiple Transitions in Semi-Crystalline Polymers*, 7th Swinburne Award Address, Plastics Institute, London, Nov. 1972.
36. Y. Kawamura, S. Nogai, J. Hirose and Y. Wada, *J. Polym. Sci.*, A2, (7), 1559 (1969).
37. Y. Ishida, *J. Polym. Sci.*, A2 (7), 1835 (1969).
38. Y. Hazony, Abstracts, 24th International Symposium on Macromolecules, IUPAC, pp. 89-92, Jerusalem, Israel, July 13-18, 1975. Manuscript in preparation.
39. J. Heijboer, *Mechanical Properties of Glassy Polymers Containing Saturated Rings*, Centraal Laboratorium TNO, Delft, The Netherlands, No. 435 (1972).
40. S. J. Stadnicki and J. K. Gillham, unpublished results.
41. R. F. Boyer, "Styrene Polymers - Physical Properties", *Encyclopedia of Polymer Science and Technology*, 13, 284 (1970).
42. H. Shindo, I. Murakami and H. Yamamura, *J. Polym. Sci.*, A-1, 7, 297 (1969).

43. S. Havriliak, *Polymer*, 9, 289 (1968).
44. A. Tanaka and Y. Ishida, *J. Polym. Sci.*, 12, 335 (1974).
45. J. Heijboer, *Physics of Non-Crystalline Solids*, North Holland, Amsterdam, p.231.
46. R. G. Kriste, *Small Angle X-ray Scattering*, H. Brumberger, Ed., Gordon and Breach, N. Y., 1967.
47. H. Tadokoro, Y. Chatani, H. Kusanagi and M. Yokoyama, *Macromolecules*, 3, 441 (1970).
48. M. D'Alagni, P. DeSantis, A. M. Liquori and M. Savino, *J. Polym. Sci.*, B2, 925 (1964).
49. I. Sakurada, A. Nakajima, O. Yoshizaki and K. Nakamae, *Kolloid Z.*, 186, 41 (1962).

Table 1  
 Characteristics of Stereoregular  
 Polymethylmethacrylates

	<u>Syndiotactic</u>	<u>Atactic</u> *	<u>Isotactic</u>
<u>Molecular Weight (18)</u>			
$\bar{M}_w$	83,200	105,000	2,780,000
$\bar{M}_n$	62,700	48,000	1,200,000
$\bar{M}_w/\bar{M}_n$	1.33	2.15	2.29
<u>Tactic Content (%) (18)</u>			
syndio-	70.1	50.6	0
hetero-	26.1	41.7	8.5
iso	3.8	7.7	91.5
<u>Transition Data</u>			
$T_g^\dagger$ , °K(Hz)	399 (0.68)	384 (0.67)	334 (0.81)
$T_\beta^\#$ , °K(Hz)	292 (1.25)	297 (1.24)	~280 (1.4)
$T_\beta/T_g$ , °K/°K	0.74	0.77	> 0.84
<u>Ratio of Peak Heights of the <math>T_\beta</math> to <math>T_g</math> Transition<sup>#</sup></u>			
	0.73	0.60	0.19
<u>Synthesis (18)</u>			
Initiator	fluorenyl lithium	*	phenylmagnesium bromide
$T_{\text{synthesis}}$ , °C	-70		0

†Determined from  $G'$  and  $dG'/dT$  loss data (decreasing temperature).

#Determined from  $G''$  loss data (decreasing temperature).

\*Source: Cellamer Associates (18).

Table II

Transition Data from Loss Maxima of \*  
Stereoregular Polymethylmethacrylates

PMMA	dG'/dT		G''		Δ		tanδ		α	
	Tg	Tβ	Tg	Tβ	Tg	Tβ	Tg	Tβ	Tg	Tβ
Syndiotactic	399	292	399	292	403	300	403	300	400	295
Atactic	384		384	297	388	297	388	297	384	297
Isotactic	334		334	~280	336	~285	336	~285	336	~285

\* Decreasing temperature data, °K.

## FIGURE CAPTIONS

- Figure 1. Syndiotactic PMMA. }  
Figure 2. Atactic PMMA. }  
Figure 3. Isotactic PMMA. }  
Figure 4. Syndiotactic PMMA. }  
Figure 5. Atactic PMMA. }  
Figure 6. Isotactic PMMA. }
- Logarithmic decrement and relative rigidity versus temperature, °K. Prehistory: heat to 473°K. Experiment: 473→93→473°K. Rate: 2°K/min. Data shown: 473→93°K.
- G'' (upper,+) and dG'/dT (lower,x) versus temperature, °K. Same Experiments as for Figures 1, 2, and 3, respectively. Data shown: 473→93→473°K.
- Figure 7. Syndiotactic PMMA. Effect of thermal prehistory.  
Logarithmic decrement versus temperature, °K.  
Prehistories: heat to 423°K and 473°K (same specimen).  
Experiments: 423→93°K(x), 473→93°K(+). Rate: 2°K/min.
- Figure 8. Syndiotactic PMMA. Thermohysteresis.  
K''G'' and K'G' versus temperature, °K.  
Prehistory: heat to 473°K.  
Experiment: 473→93→473°K. Rate: 2°K/min.
- Figure 9. Syndiotactic PMMA. Thermohysteresis.  
K'G' versus temperature, °K (linear scale).  
Same experiment as for Figure 8.
- Figure 10. Atactic PMMA. Effect of moisture (300,2500,10,000 ppm).  
Logarithmic decrement and relative rigidity versus temperature, °K.  
Prehistory: see text for conditioning.  
Experiment: 473→93→473°K. Rate: 2°K/min.  
Data shown: 473→93°K.
- Figure 11. Atactic PMMA. Effect of moisture (10,000 ppm).  
Logarithmic decrement versus temperature, °K.  
Same experiment as in Figure 11.  
Data shown: 333→93→333°K.

Figure Captions (con't)

Figure 12. Syndiotactic, Atactic and Isotactic PMMA.

K"G" versus temperature, °K.

Prehistory: 293→473°K.

Experiment: 473→93→473°K. Rate: 2°K/min.

Data shown: 473→93°K.

Figure 13. Syndiotactic, Atactic and Isotactic PMMA.

Relative Rigidity (K'G') versus temperature, °K.

Same experiment as in Figure 12.

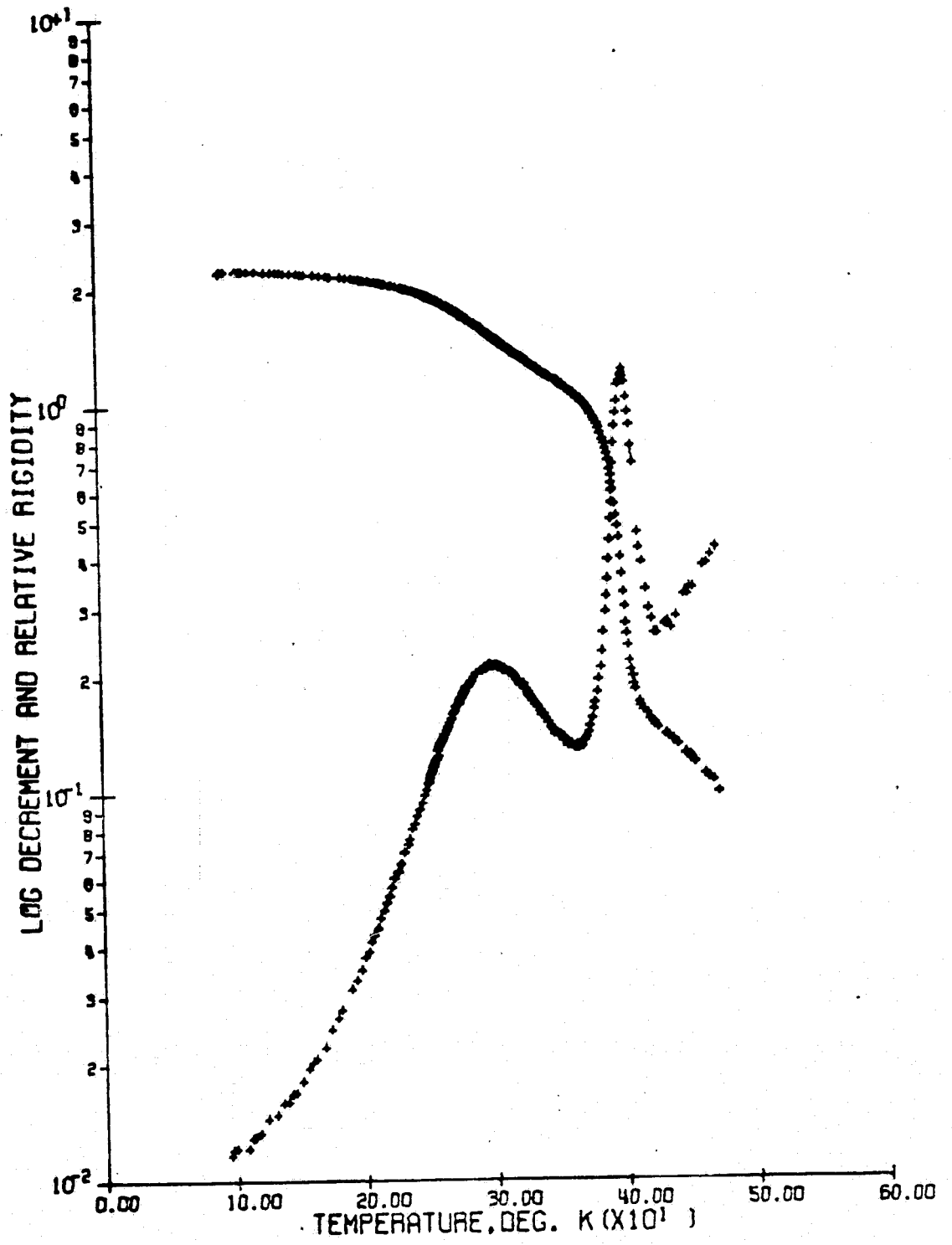


Figure 1

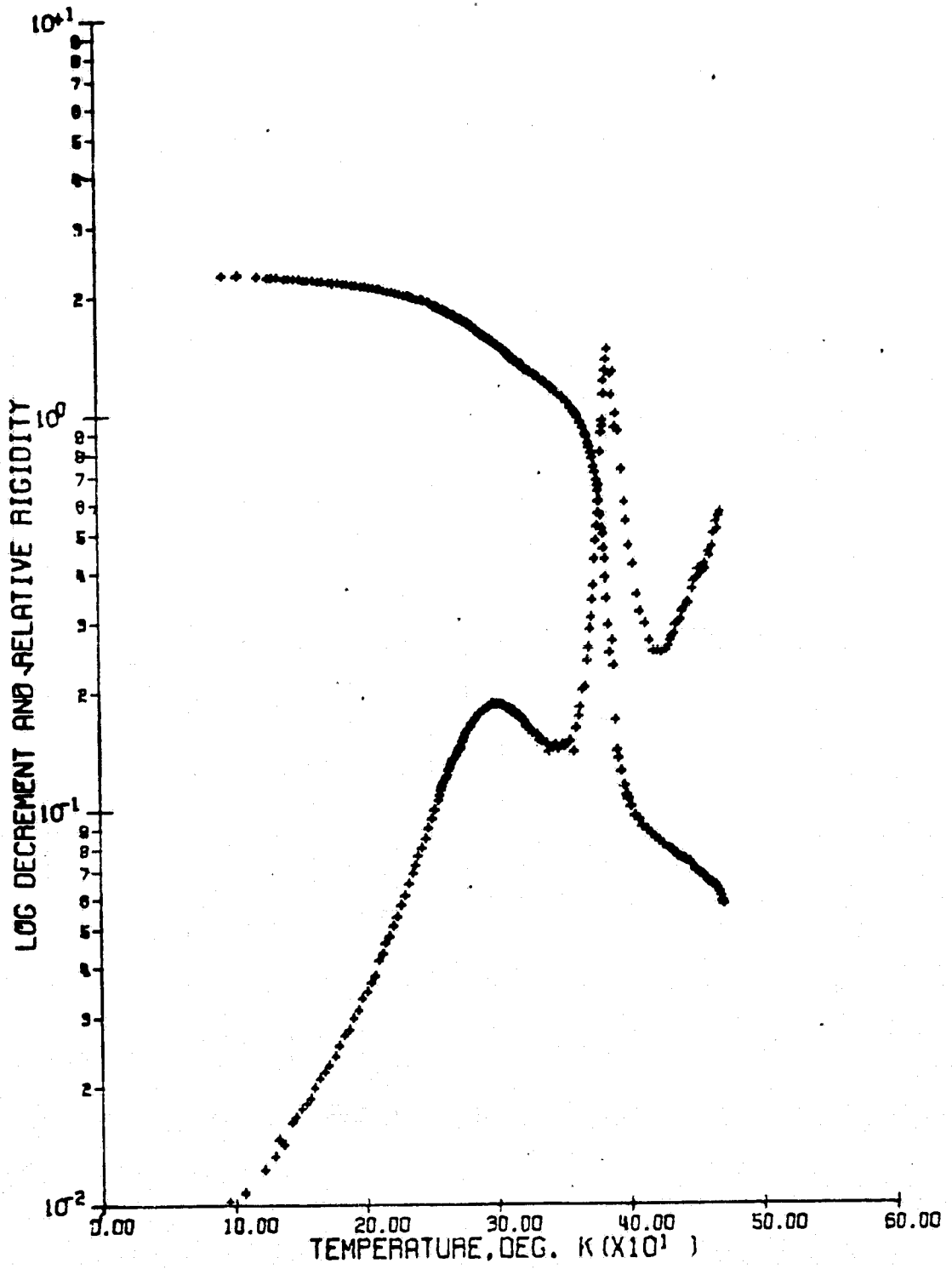


Figure 2

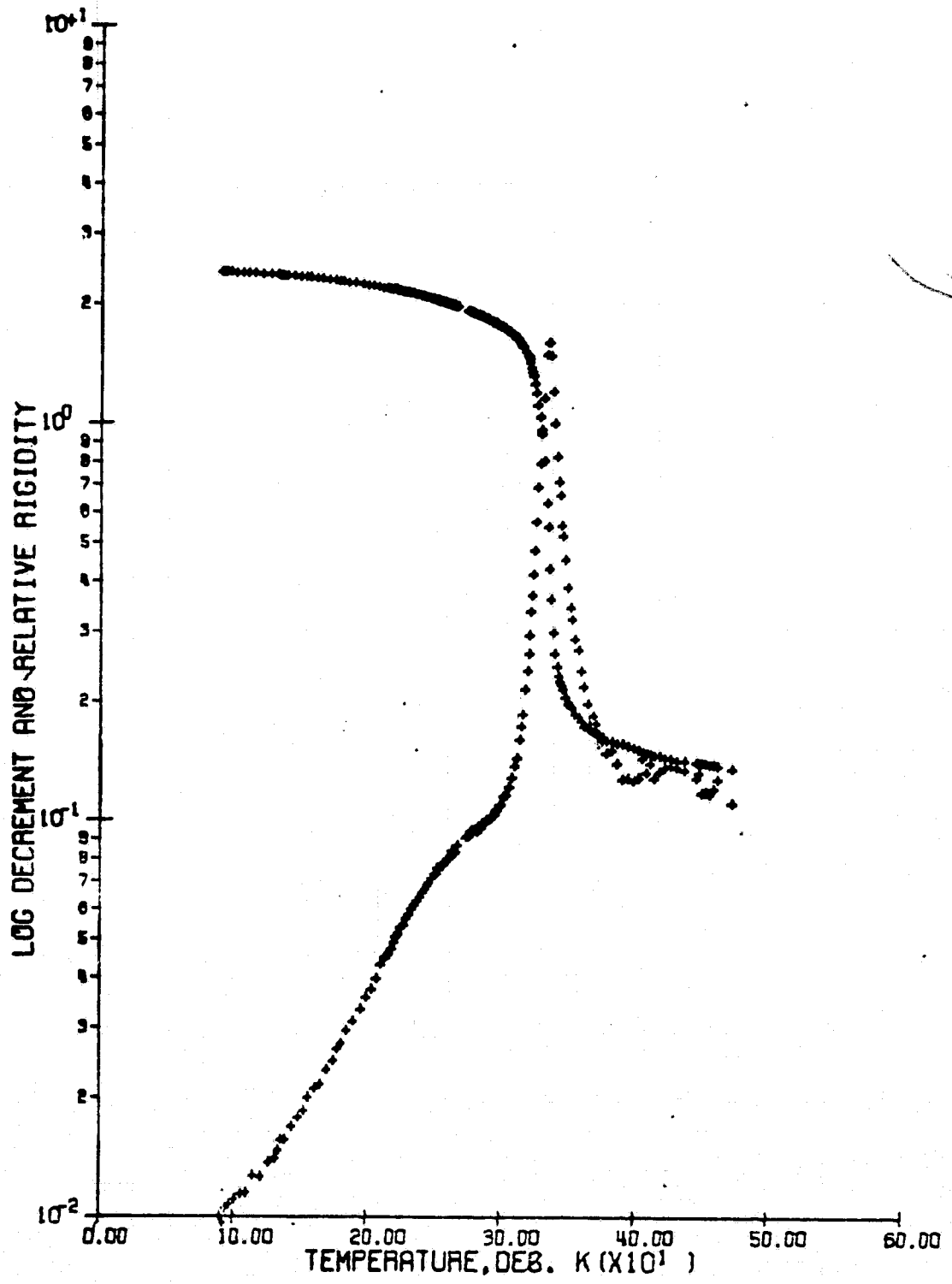


Figure 3

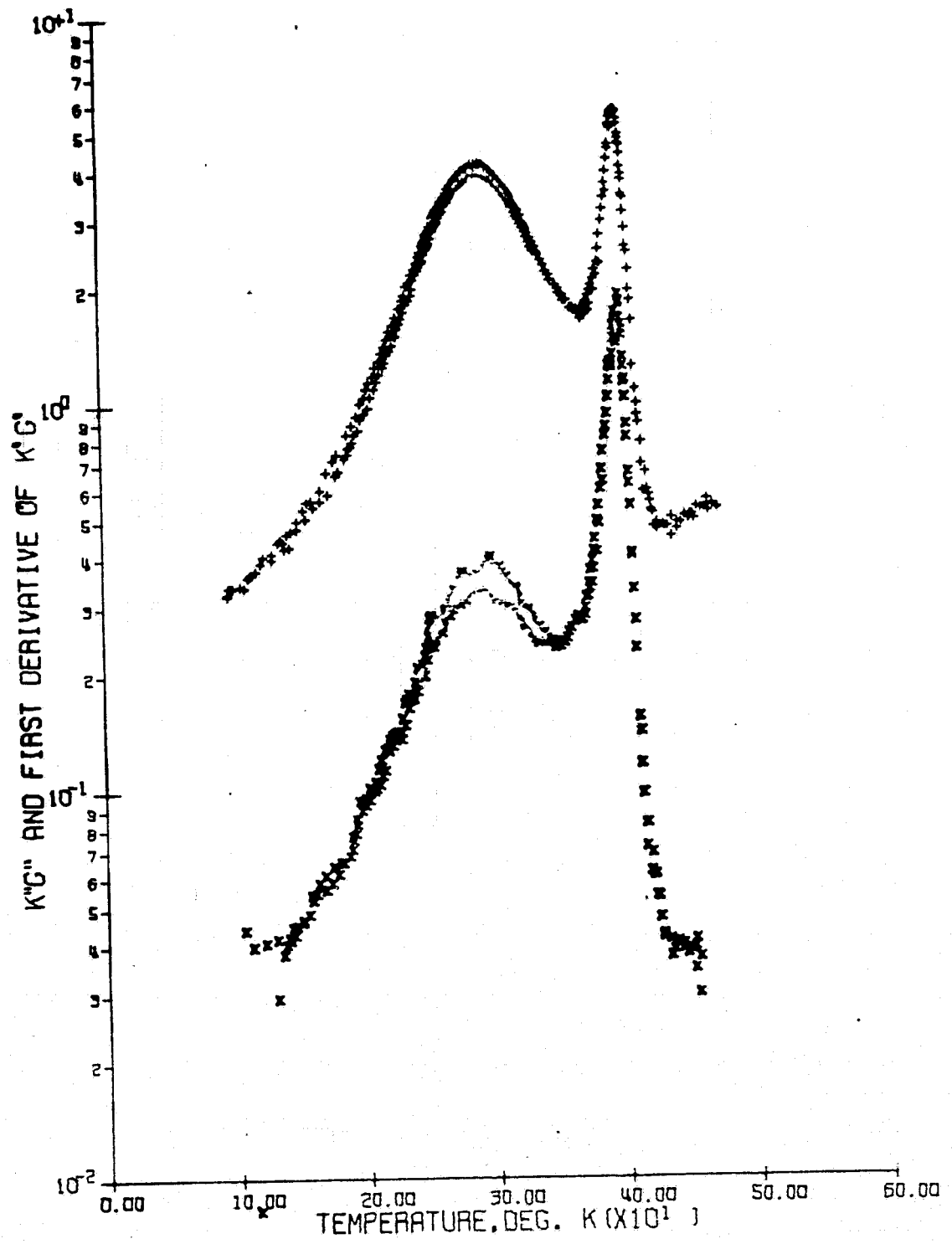


Figure 4

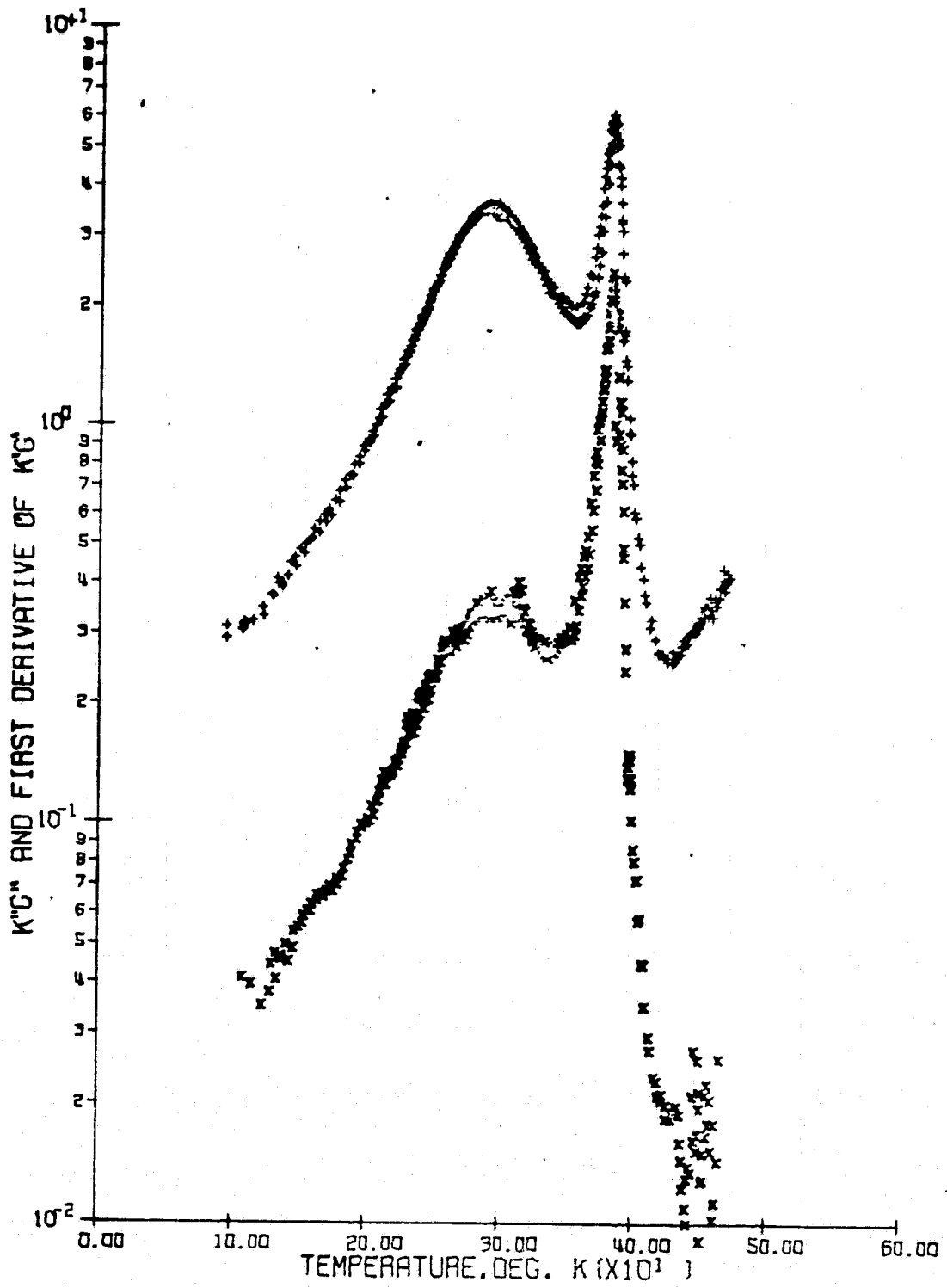


Figure 5

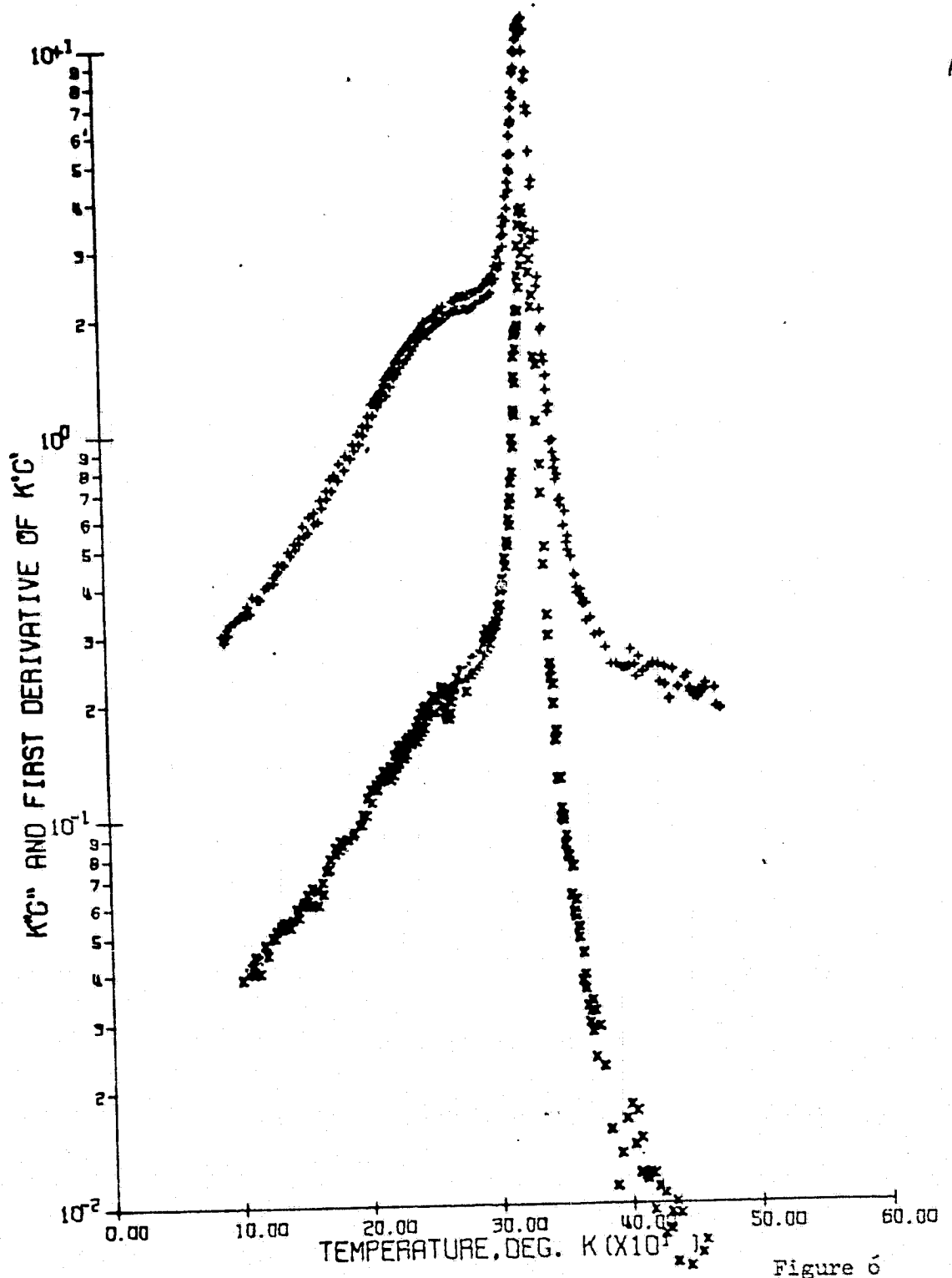


Figure 6

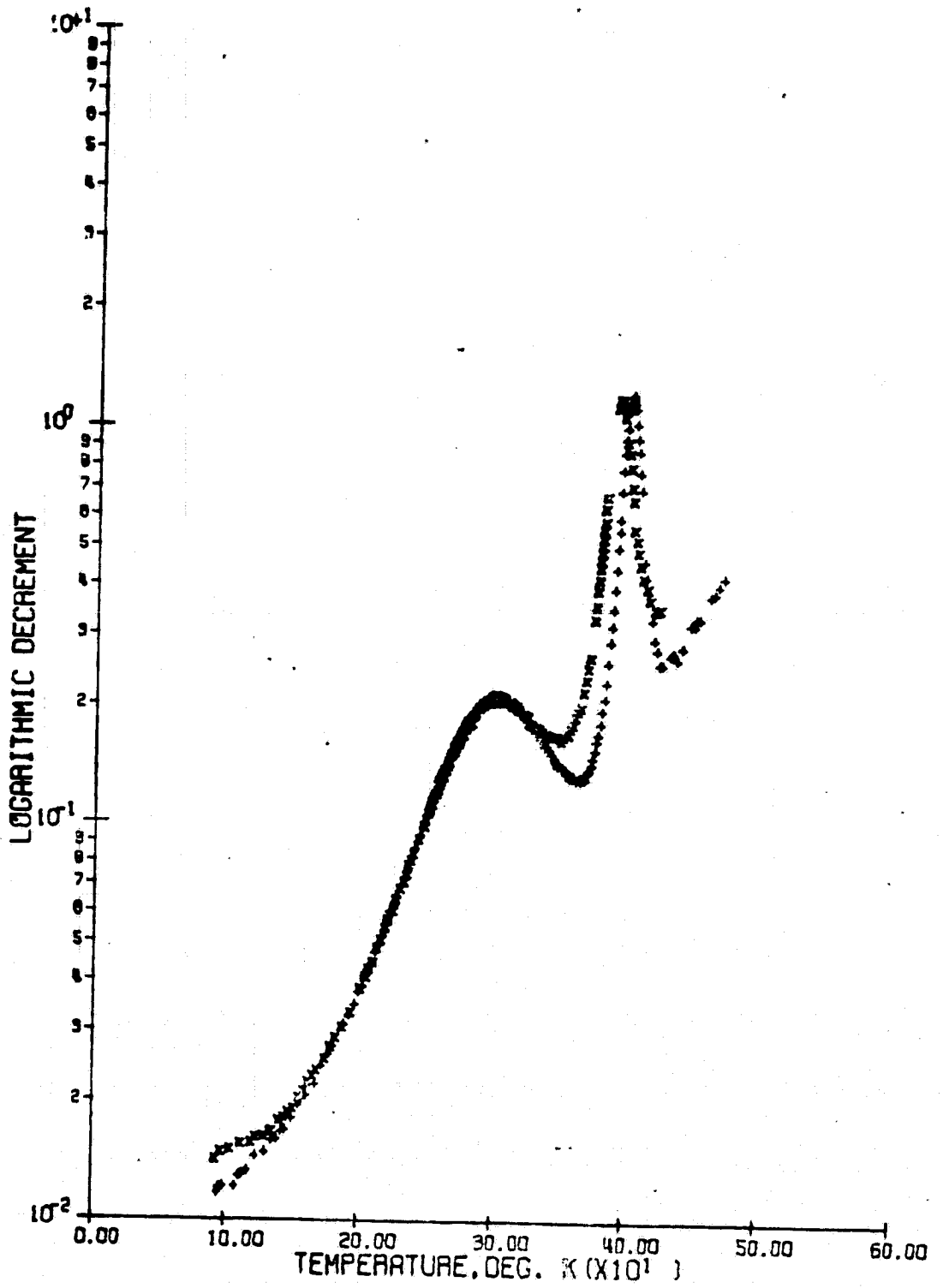


Figure 7

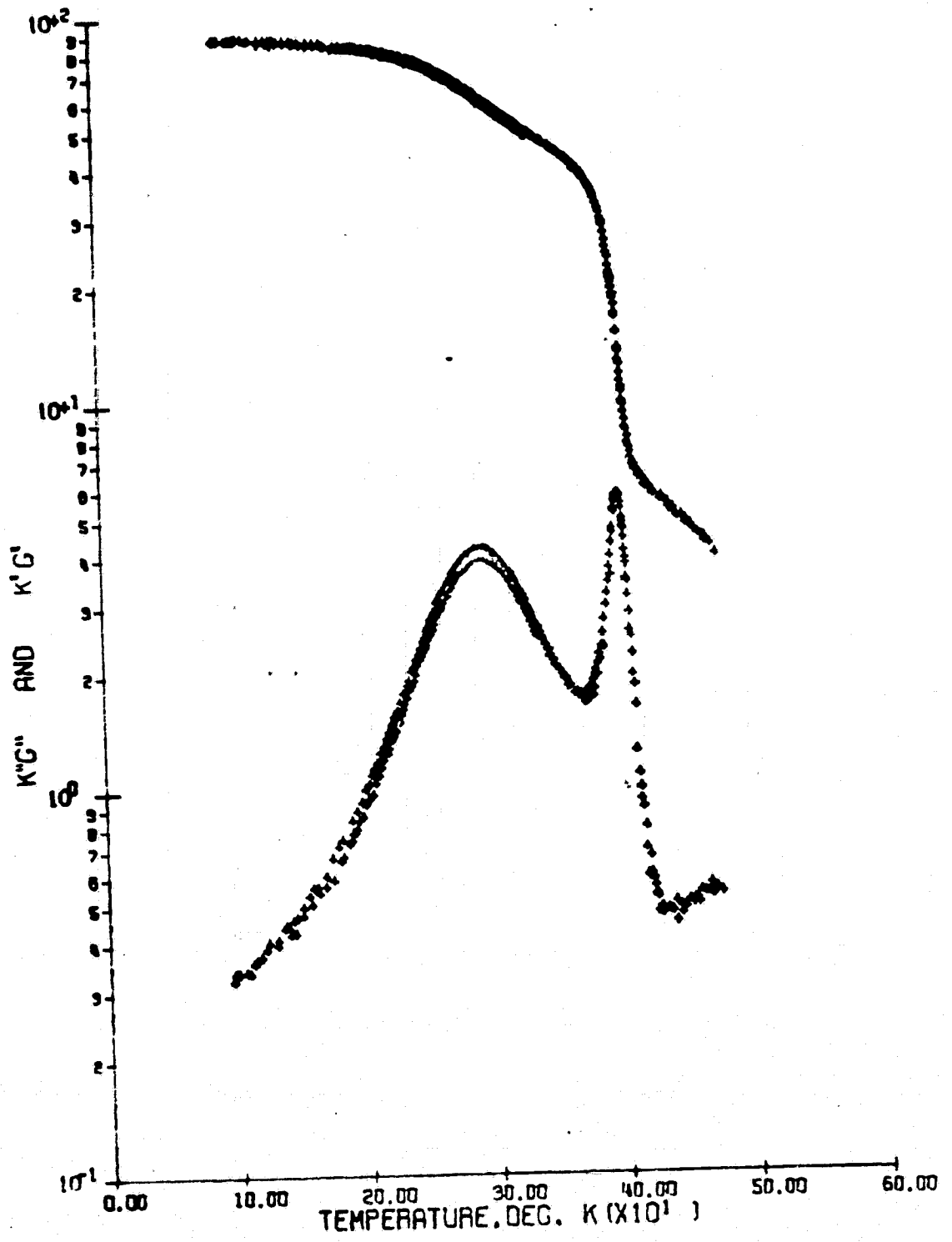


Figure 8

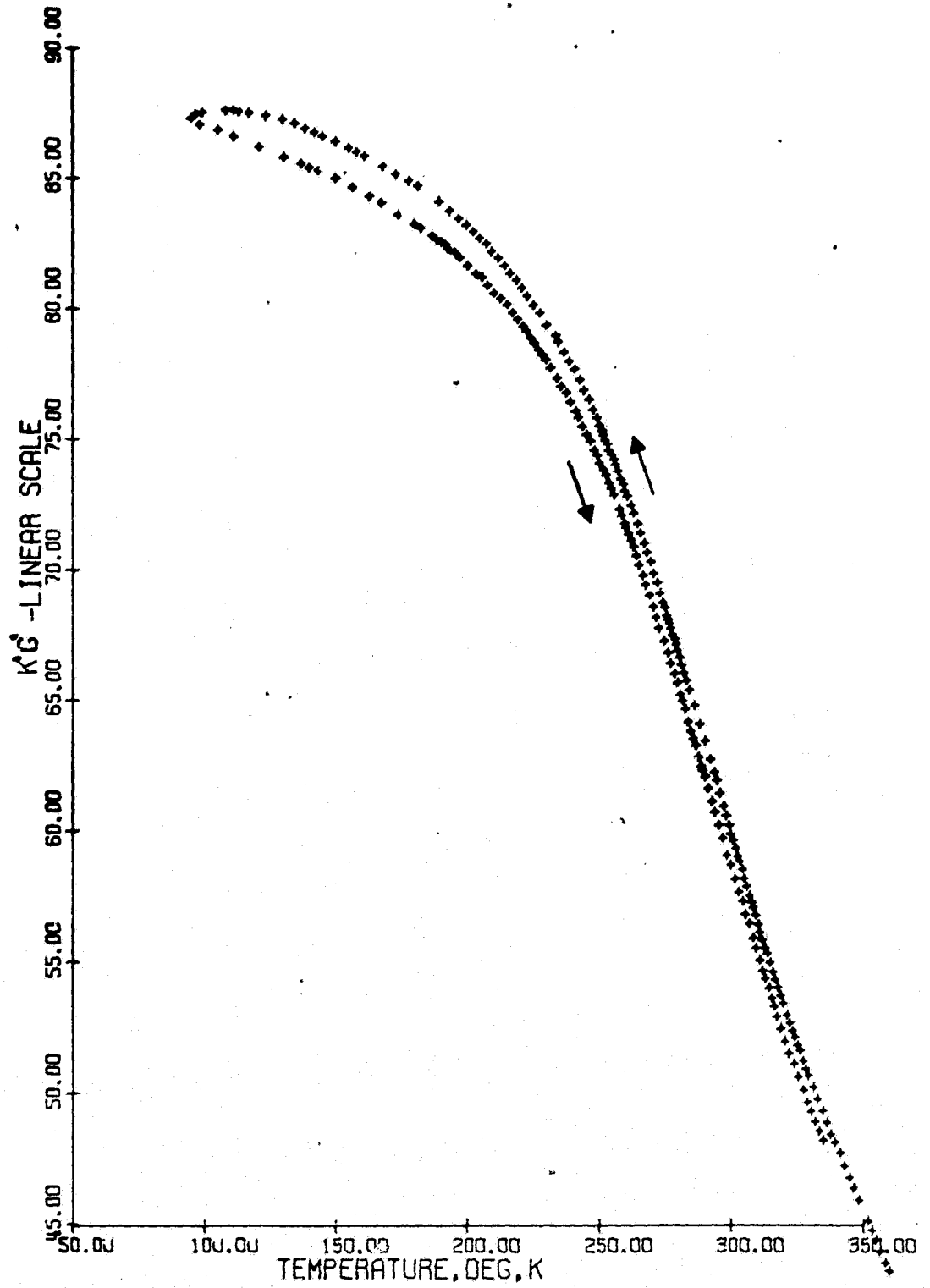


Figure 9

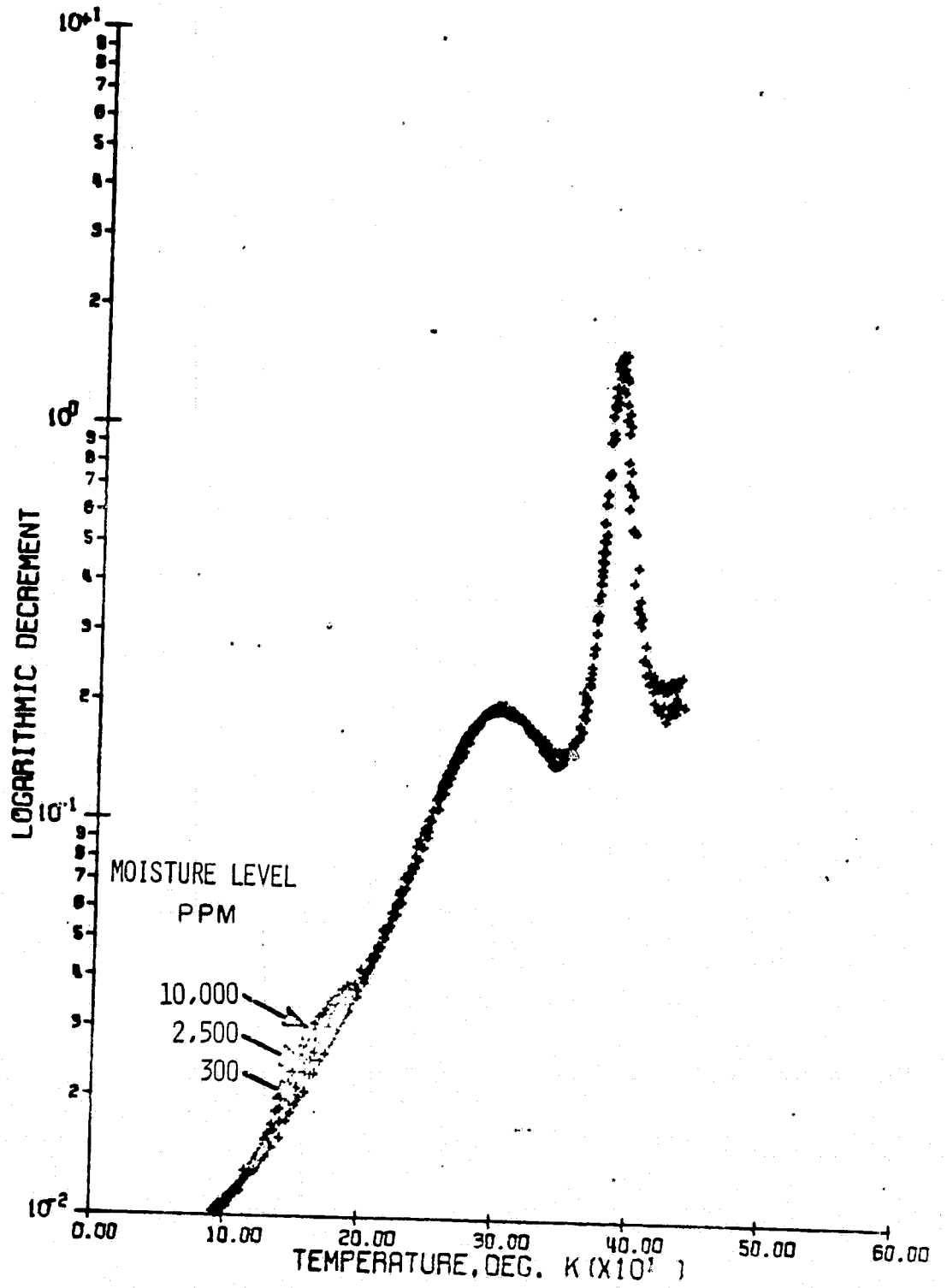


Figure 10

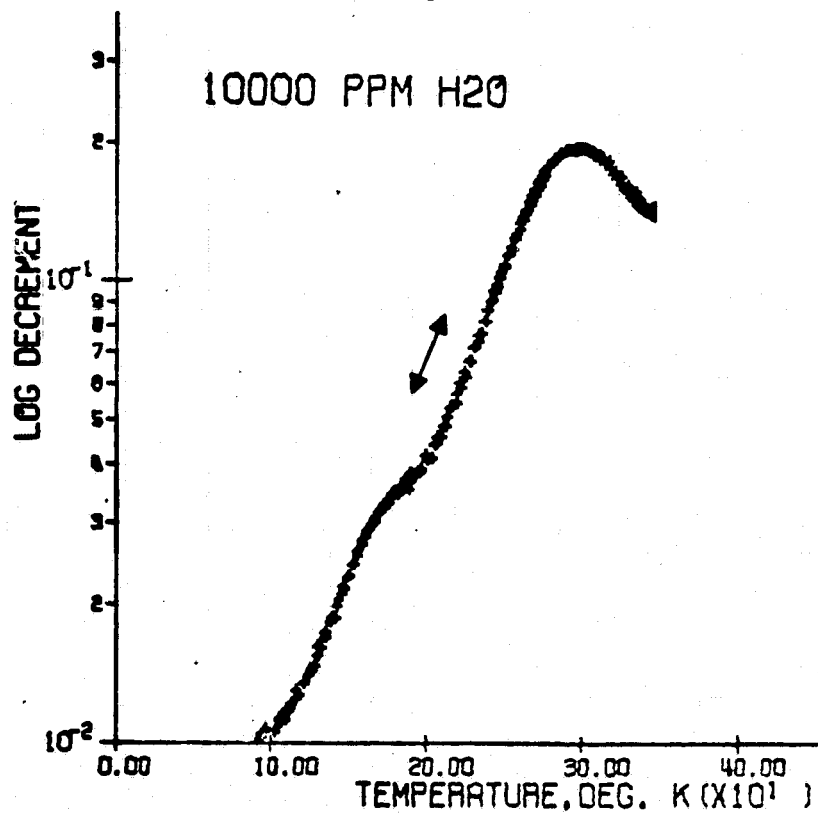


Figure 11

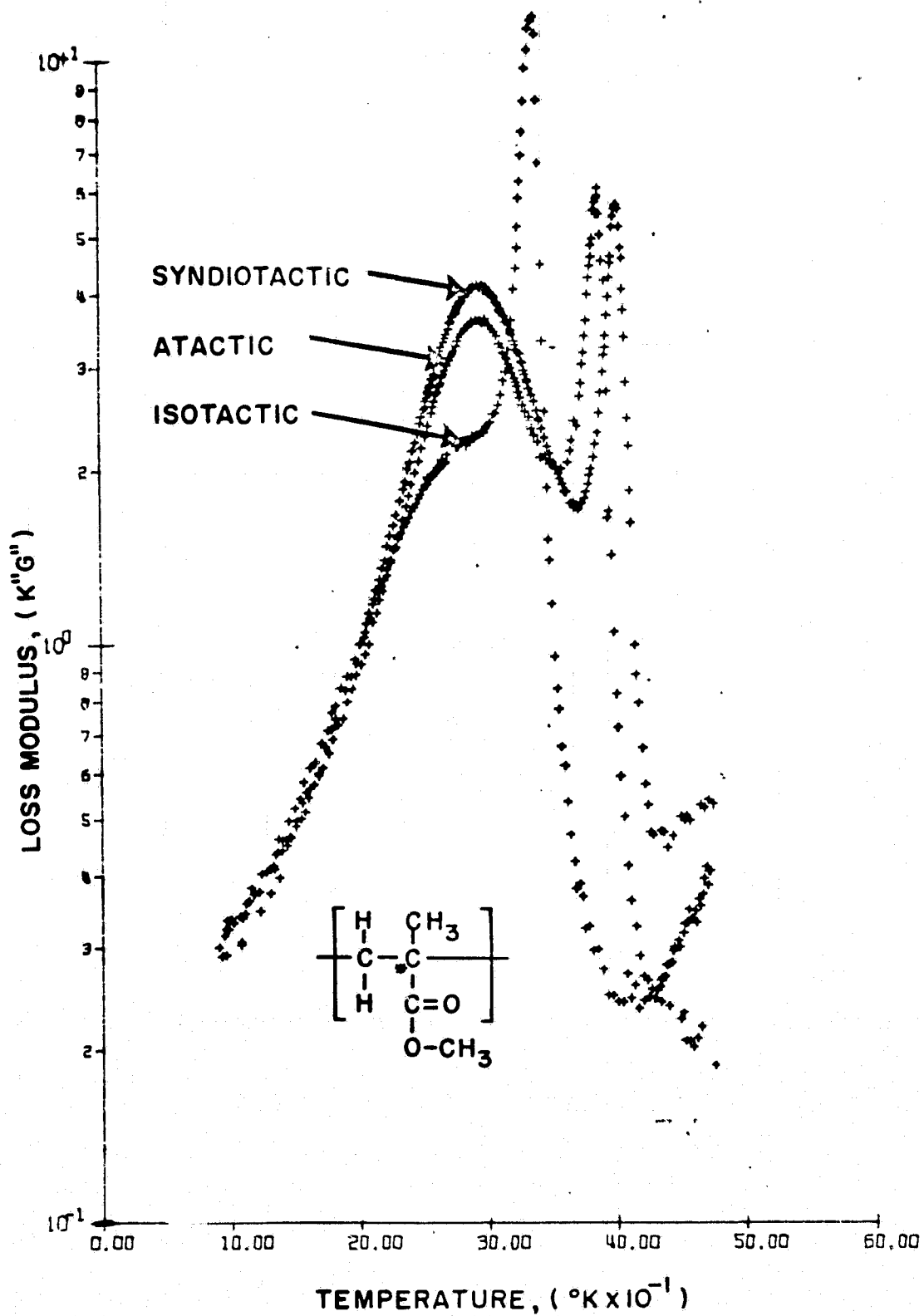


Figure 12

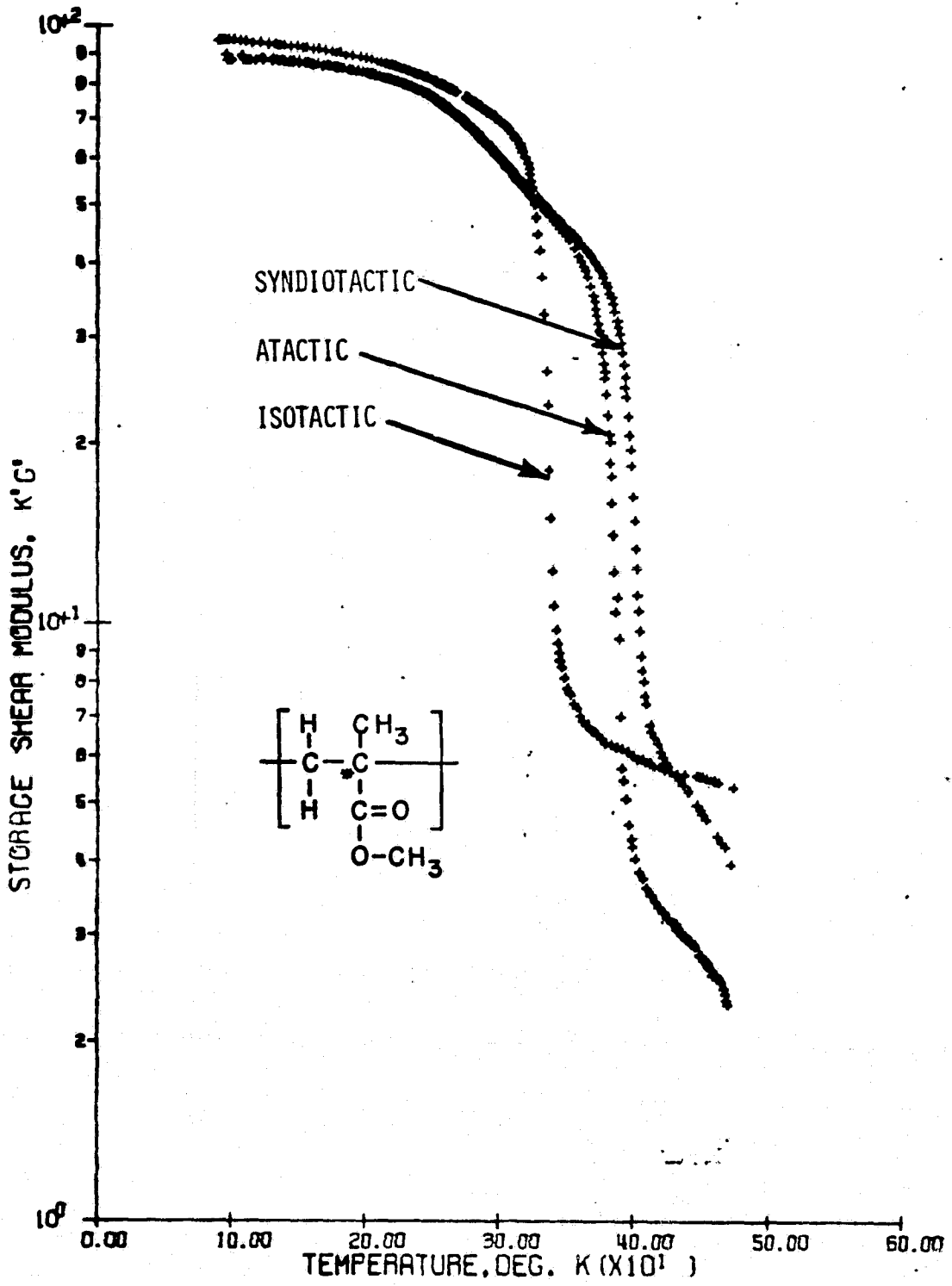


Figure 13